JOURNAL OF GEOPHYSICAL RESEARCH, VOL. 101, NO. A12, PAGES 27,077-27,090, DECEMBER 1, 1996

The 13.5-day periodicity in the Sun, solar wind, and geomagnetic activity: The last three solar cycles

Kalevi Mursula and Bertalan Zieger[1]

Department of Physical Sciences, University of Oulu, Oulu, Finland

Abstract. We make a detailed analysis of the 13.5-day periodicity of the solar chromosphere, the near-Earth solar wind, interplanetary magnetic field and geomagnetic activity during the last three solar cycles. The 13.5-day periodicity is a real quasi-periodicity whose amplitude varies sizably with time, attaining occasionally values larger than, for example, the amplitude of the 27-day periodicity. In case of heliospheric and geomagnetic variables, intervals of large 13.5-day periodicity are due to the occurrence at 1 AU of two high-speed streams per solar rotation. According to the tilted solar dipole model, such two-stream structures appear if the heliospheric current sheet is sufficiently narrow and tilted. We show that, during the main two-stream structures, the interplanetary magnetic field (IMF) indeed had a persistent two-sector structure, and the heliosheet was sizably tilted. Multiple IMF sector structure is thus excluded as the main cause for 13.5-day periodicity in solar wind and geomagnetic activity. We determine the exact time and phase (solar longitude) of all intervals of significant 13.5-day periodicity during the last three solar cycles. We find that even the longest intervals of two-stream structure (up to 2 years) consist of separate activations. Each of the main activations of the 13.5-day (as well as 27-day) periodicity has a nearly equal length of a few (about 4) solar rotations only. This gives new interesting information about the solar dynamics related to the development of the dipole tilt. Using the phase of the main 13.5-day activations, we could determine the longitudinal position of the solar dipole tilt for all major activations. We note that this position can abruptly change by even 90 deg between two successive 13.5-day activations. For each of the three solar cycles studied, the largest two-stream structures were found in the late declining phase of the cycle. On the other hand, the main activations of the 13.5-day periodicity of solar variables, which are due to two active solar longitudes approximately 180° apart, tend to occur around solar maxima.

1. Introduction

First evidence for the fact that geomagnetic activity and auroral occurrence reflect the solar rotation period of approximately 27 days were obtained already more than one century ago [*Broun*, 1876; *Veeder*, 1893; *Maunder*, 1905; *Chree and Stagg*, 1927; *Greaves and Newton*, 1929; *Bartels*, 1932, 1934]. Solar sources causing such recurrent perturbations in near-Earth space were named M regions by *Bartels* [1940]. Later, *Bruzek* [1952] and *Smyth* [1952] were among the first to note that recurrent storms are related with low coronal intensity. With the start of in situ space observations, high-speed streams and their connection to recurrent magnetic storms were detected [*Snyder et al.*, 1963]. However, only with the discovery of coronal holes [*Altschuler et al.*, 1972; *Munro and Withbroe*, 1972] and their subsequent relation to high-speed streams and recurrent storms [*Krieger et al.*, 1973; *Neupert and Pizzo*, 1974; *Hansen et al.*, 1976; *Sheeley et al.*, 1976] the long-held view of coronal holes as M regions was established. Recently, on the basis of the idea by *Dessler and Fejer* [1963] and results, for example, by *Burlaga and Lepping* [1977], *Crooker and Cliver* [1994] refined this view by emphasizing the importance of stream-stream interaction and coronal mass ejections even for recurrent magnetic storms.

Detailed studies of the 27-day periodicity of geomagnetic activity as evidenced, for example, by the long-term series of geomagnetic indices have been conducted using various power spectral [*Ward*, 1960; *Shapiro and Ward*, 1966; *Fraser-Smith*, 1972; *Delouis and Mayaud*, 1975] and correlation methods [*Sargent*, 1986]. In addition, direct observations of recurrent high speed streams in solar wind exist since early space age [*Snyder et al.*, 1963; *Gosling and Bame*, 1972; *Sawyer*, 1976].

When examining periods shorter than solar rotation period, spectral peaks at about half the solar rotation period, 13-14 days (to be called here 13.5-day periodicity for simplicity), have persistently appeared, for example, in studies of geomagnetic activity using global indices [*Fraser-Smith*, 1972; *Delouis and Mayaud*, 1975] or individual station data [see, e.g., *Courtillot and Le Mouel*, 1988, and references therein]. In most early and even some later studies, these peaks at the second harmonic of the fundamental solar rotation period were not considered to correspond to a real physical periodicity related to certain specific heliospheric conditions but rather to be due to mathematical artefacts related, for example, to numerical effects when calculating power spectra. Such a view was taken despite the fact that very high amplitudes were often obtained for the second harmonic, or that the second harmonic peaks in the high-resolution power spectra did not correspond in period or number to those around the fundamental [*Fraser-Smith*, 1972].

Bame et al. [1976] and *Gosling et al.* [1976], when studying solar wind speed by satellite instruments, noted that long intervals can exist with two high-speed streams per solar rotation. Such a persistent two-stream structure was particularly clear in

[1]Permanently at Geodetic and Geophysical Research Institute, Sopron, Hungary.

Paper number 96JA02470.
0148-0227/96/96JA-02470$09.00

1973-1975. *Fenimore et al.* [1978] studied the recurrence properties of the SW speed in detail and found that the 13.5-day periodicity can be far more dominant than the fundamental 27-day periodicity in the annual SW speed power spectra. They also noted the great variability in these power spectra from year to year, both in the absolute and relative power of the 13.5-day periodicity and the various peaks observed around 27 days. Actually, all single peaks around 27 days were only marginally significant, while the 13.5-day peak was dominant and undoubtedly statistically significant (up to 60 times above the background). *Fenimore et al.* [1978] also explained the 13.5-day periodicity in terms of two high-speed SW streams, approximately 180° apart in solar longitude.

More recently, *Gonzalez et al.* [1993] studied power spectra of the Ap index in 1932-1982 and found a dominant peak at 13.7 ± 0.4 days. They also studied 4-5 years long periods separately in sunspot maximum and late declining to minimum years and found, for example, that the second harmonic (13.5-day periodicity) dominates over the fundamental in the 4-year period from 1972-1975. However, they suggest that while the intervals which are dominated by the fundamental 27-day periodicity correspond to the two-sector IMF structure, the ones dominated by the second harmonic are due to more complex IMF sector structures.

As to the Sun, *Ward and Shapiro* [1962] were the first, after an earlier note by *Kiepenheuer* [1953], to identify the 13-day periodicity in several solar parameters, for example, in the calcium K line plage data and sunspot area and number. It was also soon realized that the nonsinusoidal nature of the 27-day periodicity can cause artificial power at the harmonics. This problem (and the acclaimed inherent 13-day smoothing of solar data) made some early researchers to deny the existence of two active solar longitudes [*Shapiro*, 1965a, b]. Typical for the controversy that still existed in early 1980s due to the varying power of the 13.5-day periodicity, different research groups, while studying the same solar parameter (e.g., CaK plage index) but for different time intervals, came to opposite conclusions, either excluding the periodicity [*Stimets and Londono*, 1982] or supporting it [*Donnelly et al.*, 1983; *Singh and Prabhu*, 1985; *Donnelly et al.*, 1985, 1986; *Donnelly*, 1988].

Nowadays, the dynamic nature of the 13.5-day periodicity of solar activity is better understood, and intervals are found where the 13.5-day periodicity is clearly visible even in time series, the spectral power greatly surpassing that of the 27-day periodicity [*Donnelly and Puga*, 1990]. *Donnelly and Puga* [1990] made an extensive study of the solar 13.5-day periodicity at several wavelengths and found that the power of the 13.5-day periodicity is very dependent on the wavelength or source region. A strong overall power in 13.5-day periodicity was found in ultraviolet (175-290 nm), while at some other wavelengths no clear 13.5-day signal was identified. They explained the power and phases of the 13.5-day periodicity at the various wavelengths in terms of their optical depth and solar central angle dependence. They concluded that the strong 13.5-day periodicity comes from episodes of solar activity with two peaks per rotation, produced by two groups of active regions roughly 180° apart in solar longitude, thus proving the existence of two active solar longitudes, and verifying the earlier work by *Heath* [1973] in UV and by, for example, *Donnelly et al.* [1983, 1985], *Lean* [1984], and *Bai* [1987] in other variables and indices.

It is clear from the above discussion that the 13.5-day periodicity exists for most solar, heliospheric and geomagnetic variables, not all the time but rather as a quasi-periodicity during certain specific intervals. One of the main aims of this paper is to study systematically the occurrence and other properties of these intervals and their relation to the solar cycle phase. We will make a comprehensive analysis of most heliospheric and geomagnetic variables and a number of solar variables, covering the last three solar cycles, that is, practically the whole space age. We will show that the 13.5-day periodicity, both in solar, heliospheric and geomagnetic variables, occurs as separate enhancements or activations which last only a few (about 4) solar rotations and may be repeated one after the other.

So far, little attention has been given to compare the 13.5-day periodicities observed in the Sun, heliosphere and geomagnetic activity. In fact, some researchers [e.g., *Bobova and Stepanian*, 1994] have suggested that the 13.5-day periodicity in geomagnetic activity is due to similar periodicity in solar chromospheric variables. On the contrary, we find that the main enhancements of 13.5-day periodicity in solar chromospheric variables occur around solar cycle maxima while the enhancements in solar wind and geomagnetic activity are found mainly in the late declining phase of the solar cycle. Thus we conclude that there is no straightforward connection between solar active longitudes and the two stream structures of solar wind.

The paper is organised as follows. In section 2 the data and method are described. In section 3 we calculate and discuss the power spectra and autocorrelation and cross-correlation functions. Solar cycle variation of the 13.5-day periodicity is studied in section 4. Section 5 is divided in six sections where different issues related to the method, results, and their interpretation are discussed. Final conclusions are presented in section 6.

2. Data and Method

In this analysis we have used all hourly averaged data for the heliospheric variables (SW speed, temperature, ion density and IMF) from the OMNI database, daily sunspot numbers, and various geomagnetic indices (Kp, aa, C9, and Dst) for the period 1964-1994. Most data for 1964-1988 were retrieved from the NGDC-05/1 CD-ROM disk Solar Variability Affecting Earth published by the National Geophysical Data Center. The more recent data were obtained from the electronic database supported by the NSSDC. The daily sunpot numbers were obtained from World Data Center C for Sunspots in Brussels. Solar variables included (Ca K-line plage index for 1970-1987, GOES background X ray intensity for 1983-1994 and Mg II core to wing ratio for 1978-1988) were obtained from the NGDC on-line database.

The hourly data were further averaged to daily values and a linear trend was removed. Data gaps, which were frequent in, for example, SW and IMF data, were filled with linear interpolation for most (but not all) purposes in this paper. The effect of repetitive data gaps imposed by the IMP 8 12.5-day orbit will be discussed in more detail in section 5. Note also that geomagnetic indices and sunspot numbers did not have data gaps at all.

Power spectra were computed for the whole data set using the Welch averaged periodogram method [see, e.g., *MATLAB*, 1994]. Data was divided into 512-day long sections, overlapping by 256 days. Each section was detrended and windowed by a 512 point Hanning window. The squared magnitudes of the 512-point FFTs of all sections were averaged to obtain estimates of the power spectral densities. Autocorrelation and cross-correlation functions were also computed for the whole data set. We first removed the annual trend from the data in order to reduce the effect of solar cycle variation. (This is essential only for the solar variables.) Only those pairs of daily data points were used

where the actually measured values existed. No interpolation procedure was applied to data at this point, hereby the effect of data gaps was completely excluded when estimating these functions.

When extracting the 13.5-day periodicity to be discussed in section 4, we used a linear phase finite impulse response (FIR) band pass filter with a lower cutoff period of 13 days and a higher cutoff period of 14 days, designed using the Parks-McClellan algorithm [see, e.g., *MATLAB*, 1994]. The algorithm is used to find an optimum filter to fit the desired frequency response. The desired transition bands were selected so that there is an 8% difference in period between the pass band and the stop bands. A long filter of order 500 was used to obtain a very flat pass band with steeply falling boundaries. The attenuation in the stop band was more than 60 dB.

Since the power spectrum maximum at 13.5 days was found to be quite narrow, much narrower than the 27-day peak (see section 3), the bandwidth of 1 day is wide enough to include a very large fraction of related power. The narrow width of the activity at 13.5 days is also motivated by results of *Gosling et al.* [1977], who noted that high-speed streams rotate rigidly at about 27 days, thus rejecting a sizable effect from differential rotation. Moreover, *Sargent* [1986] found that geomagnetic recurrency is peaked at 27 days and decreases strongly for longer or shorter periods. (Note that the recurrency index defined by *Sargent* also includes the periodicity at 13.5 days.)

3. Power Spectra and Correlation Functions

3.1. Power Spectra

We have calculated and plotted the high-frequency part of power spectra (PS) in Figures 1a-1c. This part of spectrum is dominated by 27-day periodicity and its harmonics. Figure 1a depicts SW speed, temperature, ion density, and Kp index, Figure 1b sunspot number, IMF radial component in the average interplanetary magnetic field (IMF) direction (rotated by 44 deg off the x axis in x,y plane, to be called the "sector component"), IMF z(GSM) component and the (positively definite) IMF radial magnitude, and Figure 1c Ca K-line plage index, GOES background X ray intensity and Mg II core to wing ratio.

Spectra shown in Figure 1 have very different relations between the fundamental 27-day periodicity and its harmonics, for example, the sunspot number PS (Figure 1b) shows a very strong peak at fundamental, the second harmonic being sizably suppressed (by nearly 1 order of magnitude) and subsequent higher harmonics hardly visible. On the other hand, the SW speed PS (Figure 1a) has its highest power at 13.5 days. The 13.5-day peak is very sharp, contrary to the fundamental which has a broader spectrum. Even higher harmonics, at least up to the fifth harmonic are seen in the SW speed PS, again in difference to sunspot SP. Their power seems to decrease steadily according to the 13.5-day, not the 27-day peak. (The ratio of two successive harmonics is about 2-3, the suppression being thus smaller than in case of sunspots.) These properties of SW speed PS demonstrate that the 13.5-day periodicity is another fundamental periodicity for this parameter, in addition to 27 days.

A pattern similar to SW speed was also found for power spectra of SW temperature and ion density, Kp index (Figure 1a), and radial IMF magnitude (Figure 1b) (as well as total IMF and aa and C9 geomagnetic indices which were not depicted in Figure 1). However, the IMF z component (given in GSM coordinate system in Figure 1b) has dominant power at around 27

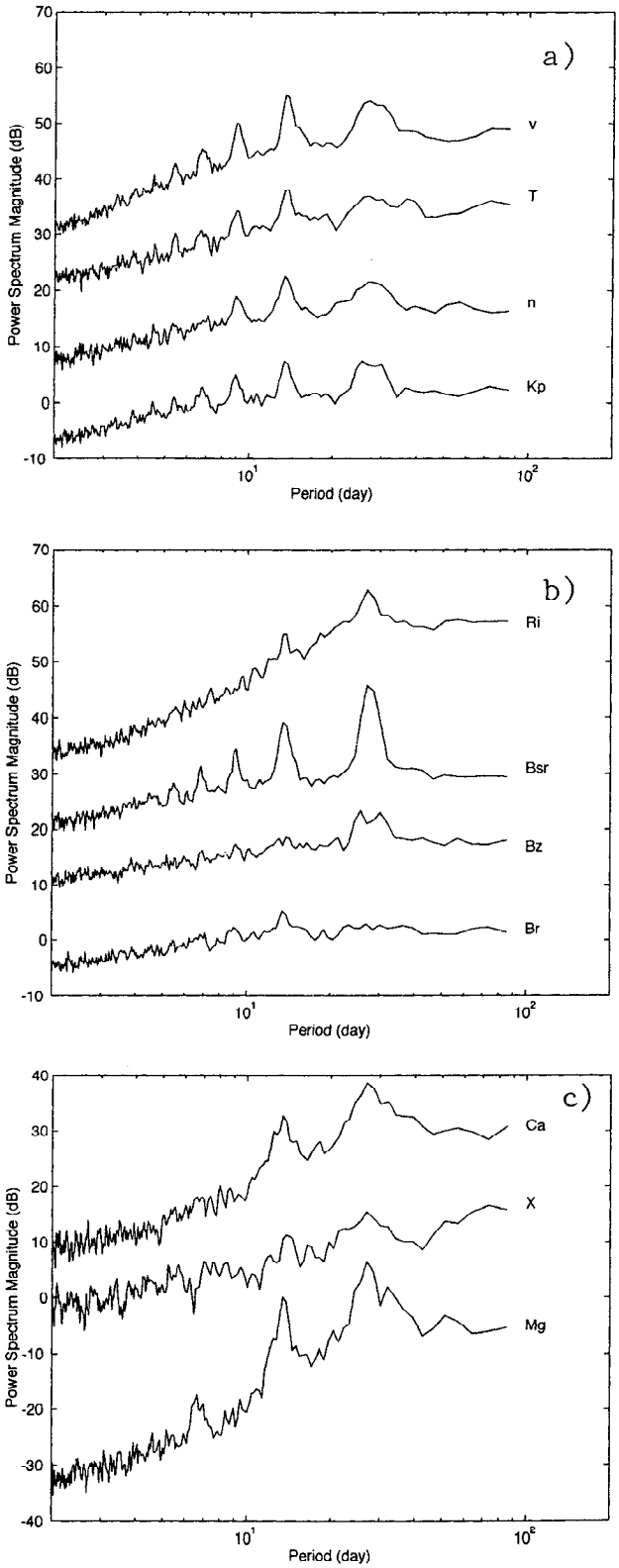

Figure 1. High-frequency part of power spectra for (a) SW speed (v), temperature (T) and ion density (n) and geomagnetic Kp index; (b) sunspot number (Ri), IMF radial component in the average IMF direction (Bsr), IMF z(GSM) component (Bz) and IMF radial magnitude (Br); (c) Ca plage index, X ray intensity, and Mg ratio. Horizontal axis gives the period in days on a logarithmic scale. Scale of the logarithmic vertical axis is given in decibels, but the absolute level is arbitrary.

days. The second harmonic is fairly weak with respect to the fundamental, and higher harmonics are hardly visible. In this respect the IMF z component PS resembles that of sunspots but the suppression of harmonics is smaller. Similarly, the IMF sector component PS (Figure 1b) has its strongest peak at 27 days, but harmonics up to at least the fifth are clearly visible in PS. Thus the sector component is more efficient than the z component when studying multiple IMF sector structures.

All the three solar variables (Figure 1c) have dominant power at 27 days, but the 13.5-peak is fairly strong too. Note also that power spectra of the two upper solar variables in Figure 1c show, similar to sunspot PS, practically no evidence for peaks at higher harmonics. This shows that these variables do not have three or more simultaneously active longitudes and that these variables change fairly sinusoidally, producing little power in higher harmonics. However, there is a clear peak in the Mg spectrum at about 6 days, that is, at the fourth harmonic of the fundamental or rather the second harmonic of the 13.5-day periodicity, which is probably due to the nonsinusoidal nature of the 13.5-day periodicity.

3.2. Autocorrelation Functions

Figures 2a-2c depict autocorrelation functions (ACF) for the same variables whose power spectra were plotted in Figures 1a-1c. Sunspot number ACF (Figure 2b) shows the expected occurrence of correlation peaks for multiples of 27 days due to long lasting sunspot regions. Such a repetition in sunspot numbers is seen to extend up to 8 solar rotations, ending fairly abruptly thereafter. Thus the lifetime of the most persistent sunspot regions is about 8 solar rotations. However, most importantly for the present study, the sunspot number ACF does not show evidence for periodicities shorter than 27 days.

Again, results are different for the ACFs of many other variables, for example, the SW speed ACF (Figure 2a) shows a periodicity peak for multiples of 13.5 days. The peaks of the first 13.5-day multiples are very regular, but beyond about 4 solar rotations the peaks get distorted by intensity and phase changes. However, the 13.5-day multiple peak pattern is seen to extend over the whole coherency length studied, at least for 1 year. Note also that the cancellation of coherency beyond 8 rotations is not seen in SW speed. There is also clear evidence in SW speed ACF for enhanced 27-day recurrency which lasts for about 3-4 solar rotations with constantly decreasing intensity, then dying out to the level of 13.5-day periodicity. Similar recurrent peaks at 2-3 times the solar rotation period were also detected by *Gosling and Bame* [1972] in some SW speed ACFs for 1964-1967 using direct spacecraft measurements, and by *Coles* [1978] in the ACFs of SW speed from high solar latitudes using interplanetary scintillation method. *Gosling and Bame* [1972] also noted on the strong variability of the degree of correlation in time.

Most features noted above for SW speed appear also in the ACFs of SW temperature, ion density, Kp index (Figure 2a) and IMF radial magnitude (Figure 2b). In particular, the 13.5-day multiple peak pattern is observed, either during several (as, e.g., for SW temperature) or only a few (IMF radial magnitude) solar rotations. It is quite remarkable how closely the SW temperature ACF resembles the SW speed ACF at least up to the recurrency period of one year. Furthermore, the ACFs of these parameters also demonstrate the enhanced 27-day recurrency during 3-4 solar rotations, indicating this to be a general property for solar wind, IMF, and geomagnetic activity.

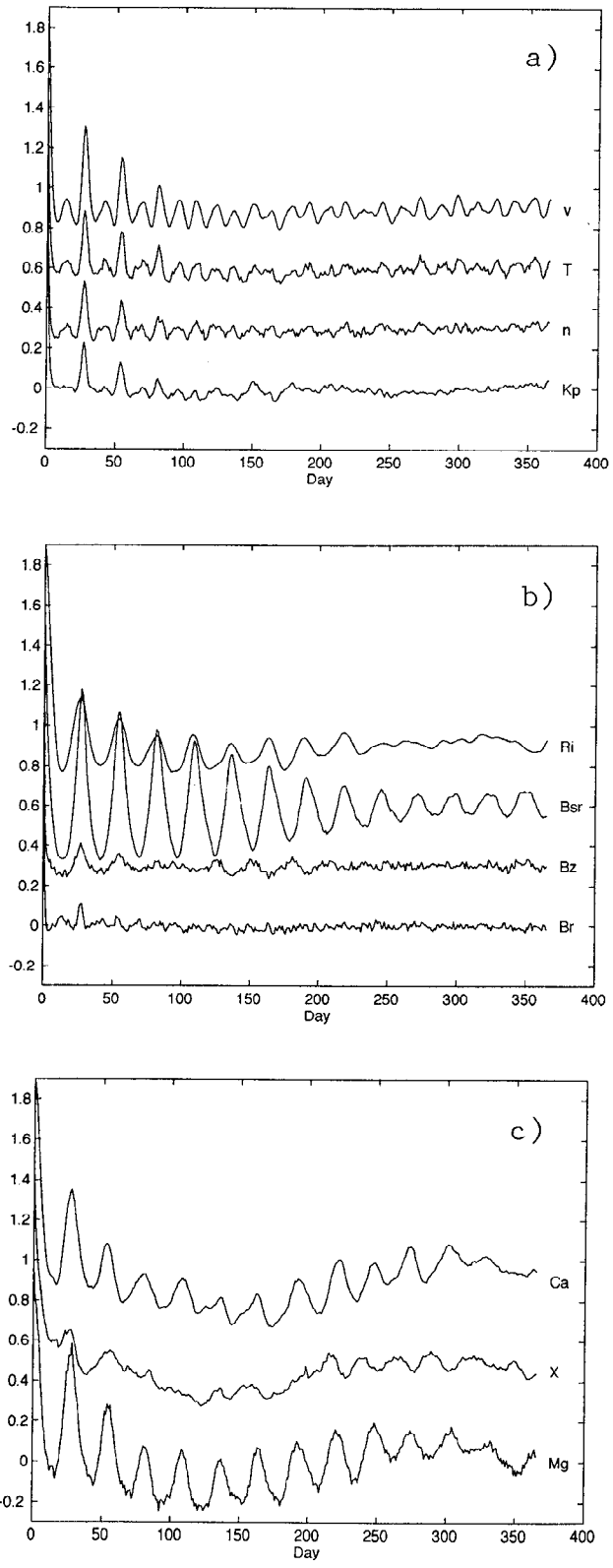

Figure 2. Autocorrelation functions for the same variables as in Figure 1. Horizontal axis gives the time lag in days. Vertical scale is valid for the lowest parameter of each figure, (a) Kp, (b) Br, and (c) Mg. Zero levels for other parameters are raised by 0.3, 0.6 and 0.9 for n, T, and v, respectively in Figure 2a; by 0.3, 0.6, and 0.9 for Bz, Bsr, and Ri in Figure 2b; by 0.45 and 0.9 for X ray and Ca in Figure 2c.

The ACFs of IMF z component and, in particular, sector component (Figure 2b) show a negative minimum between zero lag and the 27-day peak, indicating the preference of oppositely oriented IMF after half a solar rotation. This supports the overall dominance of the two sector IMF structure. However, the ACF of IMF sector component is asymmetric in the way that the first maxima are larger (in absolute value) than the minima, giving evidence for more complicated but subdominant IMF structures. It is also curious to note that this asymmetry lasts for about 8 solar rotations, that is, approximately as long as the longest coherency of sunspots. On the other hand, the solar X ray and Mg ACF's contain a small but clear peak at 13.5 days (see Figure 2c), and weak evidence for that is visible even in the Ca ACF.

3.3. Cross-Correlation Functions

We have computed the crosscorrelation functions (CCF) between SW speed and the following variables: SW temperature, ion density, radial IMF magnitude and Kp index. CCFs were calculated in two different ways. Figure 3a depicts results obtained using only actually measured values of raw data without interpolation. In Figure 3b we show the corresponding CCFs for data which were first linearly interpolated over data gaps and then filtered using the 13-14-day band pass filter. As seen in Figure 3a, maximum correlations are quite high even for raw data, in particular for SW temperature and Kp index. (The good correlation between SW speed and geomagnetic activity is known since the early SW measurements by *Snyder et al.* [1963].) However, the maxima of all CCFs, especially those for ion density and radial IMF, are higher in Figure 3b than in Figure 3a. This enhanced cross-correlation and all other differences between the two groups of CCFs are due to filtering which diminishes the effect of random noise and other signals in raw data. (We have also calculated CCF's using linearly interpolated raw data. Their maxima were slightly smaller but their shapes were similar to those in Figure 3a. Thus linear interpolation tends to decrease, not increase cross-correlations and, consequently, the higher correlations found for the filtered data are not due to linear interpolation.)

Interesting phase differences (i.e., time lags) between SW speed and the other variables can be seen in Figures 3. Except for ion density, all variables seem to have their CCF maxima earlier than SW speed ACF. The correlation between SW speed and ion density is negative (around zero lag), and the minimum in ion density comes 1 day after the SW speed maximum. These phase differences are observed both in raw data (Figure 3a) as well as in filtered data (Figure 3b). However, the phase differences stand out more clearly in filtered data than in raw data, in particular for radial IMF magnitude where a time lag of 3 days is observed for filtered data. The phase shifts will be discussed in more detail in section 5. (We have examined the reliability of the positions of correlation maxima, i.e., phase differences, using Fisher's transformation, and Student's test and found that they are valid to 99% confidence level.)

We have also calculated cross-correlations for all other pairs of the three SW variables, IMF radial magnitude, and Kp index and obtained similar results and conclusions for them as seen in Figures 3. For each pair of these variables, CCFs of filtered data

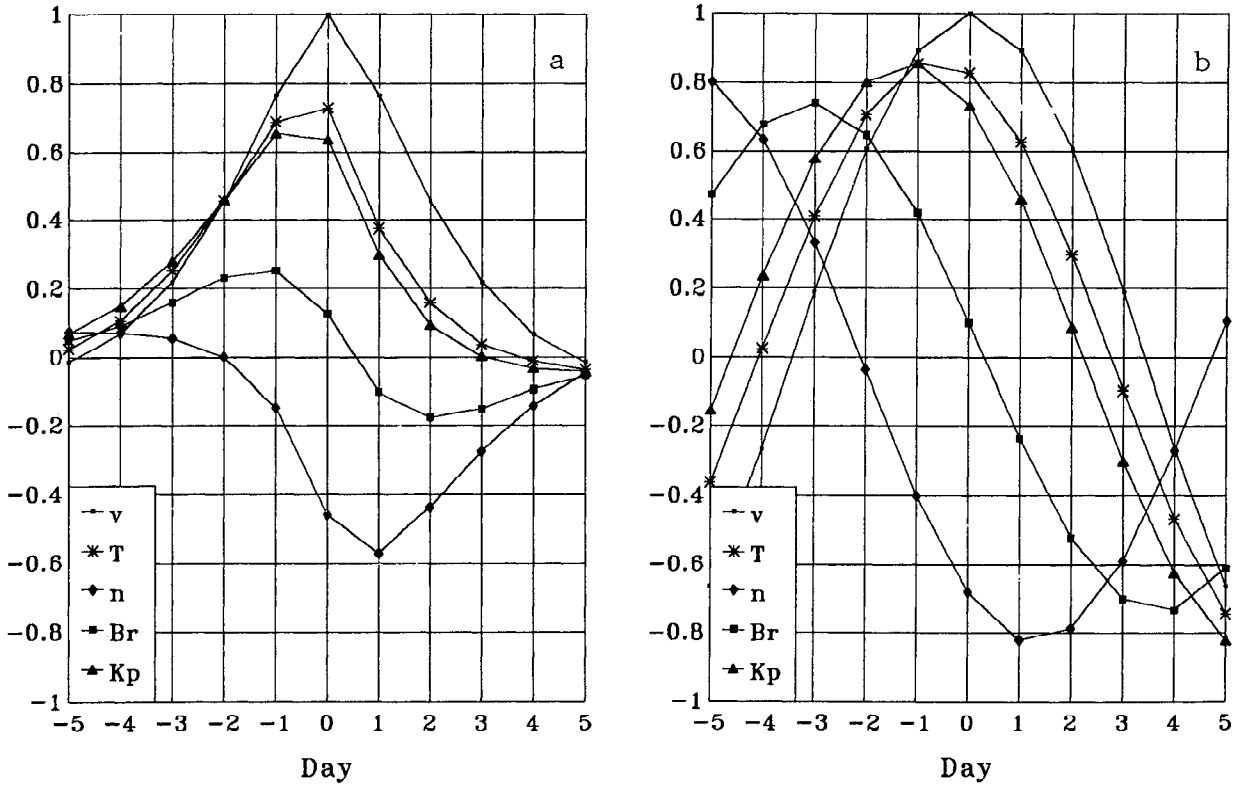

Figure 3. Cross-correlation functions between SW speed and following parameters: SW temperature (star), ion density (diamond), IMF radial magnitude (square), and Kp index (triangle) using (a) raw data; (b) linearly interpolated and 13.5-day filtered data. SW speed autocorrelation function (dot) is added in both parts for comparison.

were higher than those of raw data. We have also calculated cross-correlations between these variables and the two IMF components as well as sunspot numbers. No enhancement was found for these CCFs when using filtered data. Furthermore, CCFs between sunspot numbers and all other variables were found to be insignificantly small and remained so after filtering.

4. Solar Cycle Variation of the 13.5-Day Periodicity

We have calculated the 13.5-day periodicity over the whole data period by filtering data using the band pass filter described in section 2. The resulting 13.5-day periodicity variations (normalized to standard deviations in order to allow comparison between different variables) are displayed as color intensity maps in Plates 1a-1c for the same parameters that were studied in Figures 1a-1c and 2a-2c. In Plate 1, the 13.5-day periodicity for one Carrington rotation (27.2753 days) is plotted along vertical axis so as to demonstrate the occurrence of 13.5-day maxima and minima in heliographic longitude. (To obtain these maps, we had to interpolate the daily data with a sampling interval of 27.2753/27. Note also that we did not subtract the constant delay time due to SW propagation to 1 AU.) Furthermore, sunspot numbers averaged over one Carrington rotation are added on top of Plates 1a-1c in order to give a reference for discussion on the solar cycle phase. The same color scale was used in all plots, red and blue representing high positive and negative values of the 13.5-day periodicity, and light green representing values around zero. (Color scale ranges from -1.3 to 1.3 times the standard deviation of respective raw data.)

It is remarkable how similar a pattern is seen in Plate 1a, persisting over the whole interval, between the three SW variables and Kp index. This strongly supports the usefulness of the method and verifies, for example, the high cross-correlations found above for the 13.5-day filtered variables. The overall 13.5-day intensity is slightly higher for SW speed and temperature than for ion density and Kp index, in agreement with the higher 13.5-day power seen in the respective power spectra (Figure 1a) and ACFs (Figure 2a). Plates 1a and 1b also depict the (nearly) opposite phase between ion density and SW speed, as well as other phase differences (time lags) seen in the CCFs. (Phase differences will be further discussed in section 5.)

In Plate 1a, enhanced 13.5-day periodicity amplitudes are observed nearly always at the same times and with very similar lengths for all the four parameters. Highest 13.5-day amplitudes for all these variables during the two solar cycles (SC) 20 and 21 are detected in the late declining phase. This is clearly visible for cycle 20 where a very strong enhancement from 1973 until 1975 was observed, as well as for cycle 21 where a somewhat weaker maximum occurred toward the end of 1984. This pattern is seen to continue to SC 22 but not as clearly as in earlier cycles. A few enhancements can already be observed in the declining phase of SC 22, but for most variables they are weaker than the highest maxima in earlier cycles. Furthermore, some of the variables attain their presently highest values for SC 22 during different enhancements, for example, SW temperature already in the early declining phase in 1991 and SW density late in 1992. However, since Plates 1a-1c do not cover the full cycle, it is premature to make final conclusions for SC 22. Other, less intense 13.5-day activations in Plate 1a are found in the earlier declining phase, as, for example, the two intensifications in 1982, but also at minimum, as in 1976 and 1986, and even in the ascending phase, as in 1979 and 1989.

The long two-stream SW structure in 1973-1975 was already discussed by *Bame et al.* [1976], *Gosling et al.* [1976] and *Fenimore et al.* [1978]. We can now resolve the detailed structure of this interval to consist of 5-6 separate activations. The first two activations occur in 1973, the latter being in a clear phase difference with all other activations. (We will discuss this phase difference in section 5.) The 3-4 last activations from early 1974 until mid-1975 closely follow each other in time and have nearly the same longitude. Two of these activations are among the largest for SW speed during the whole 30-year period studied. The strength and coherence of this chain of activations caused the extremely high 13.5-day peak in SW speed power spetrum in 1974 found by *Fenimore et al.* [1978]. The small phase (longitude) difference between the subsequent activations of this chain, now verified in detail, concentrates the power into one single peak, rather than spreading it over a range of periods [*Fenimore et al.*, 1978]. Note also that the small decline in longitude starting from the first activation in 1973 and including the main chain of activations in 1974-1975 indicates that the actual rotation period of the two-stream structures was very close but slightly smaller than the Carrington period of 27.2753 days. This agrees with the result that the high-speed streams rotate at a fixed period of about 27 days [*Gosling et al.*, 1977].

The 13.5-day periodicity plots depicted in Plates 1b and 1c look quite different from those in Plate 1a (excluding SW speed which is repeated in Plate 1c). Only IMF radial magnitude shows some similarity with the general pattern of Plate 1a, with most dominant and subdominant enhancements of Plate 1a seen there as well. However, the overall intensity of IMF radial magnitude remains below that of Plate 1a, and the relative amplitudes of the 13.5-day enhancements in IMF radial magnitude are different from those depicted in Plate 1a; for example, the main activations of Plate 1a in 1973-1975 and 1984 are not among the strongest enhancements for IMF magnitude. Instead, the IMF radial magnitude has more power during other phases of solar cycle than the variables of Plate 1a. This is true, for example, for the enhancements in the ascending phase in 1978-1979, in the early descending phase in 1982 and 1992 and the maximum of SC 20 in 1970 and SC 22 in 1989-1990. (We will discuss the IMF radial magnitude in more detail in section 5.)

The two IMF components in Plate 1b show very different patterns compared to all other plots in Plate 1 and attain quite different intensities with each other. The overall intensity of IMF z component is rather low, demonstrating again the difficulty in using this parameter for possible IMF sector analysis. However, the main 13.5-day enhancements seen in z component do coincide well with simultaneous activations in IMF sector component. The sector component has several fairly strong 13.5-day activations which denote intervals of four sector IMF structures. Most interestingly, four sector structures do not generally coincide with the two stream structures of Plate 1a; for example, the largest 13.5-day enhancements of IMF sector component are in 1968, 1978, and especially in 1980-1981 and 1983-1984, when the simultaneous intensity in Plate 1a was minor. These enhancements are located in the ascending or early descending phase of solar cycle, in agreement with the previously known occurrence of multiple IMF structures. Note also that enhancements in IMF sector component seem to last longer than corresponding activations in Plate 1a (see also section 5).

Solar variables (sunspot number in Plate 1b; Ca index, X ray intensity and Mg ratio in Plate 1c) all attain fairly weak overall 13.5-day periodicity intensities compared, for example, to SW speed. While sunspot number shows a rather blurred pattern

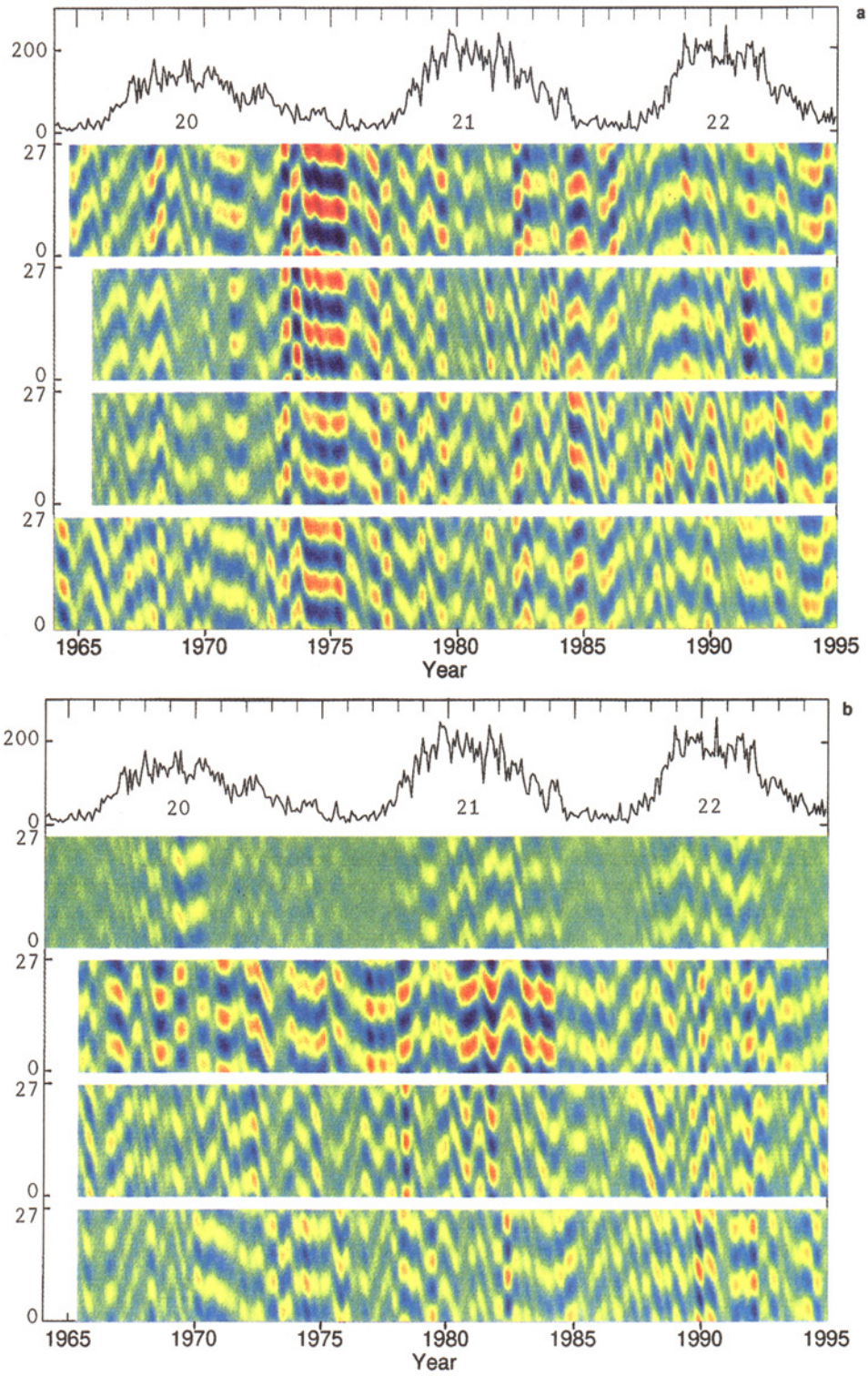

Plate 1. (top) Sunspot numbers averaged over one Carrington rotation, and the four color plots depict the 13.5-day periodicity in Carrington presentation for (from top to bottom) (a) SW speed, temperature, ion density, and Kp index; (b) sunspot numbers, IMF sector component, IMF z component, and IMF radial magnitude; (c) SW speed, Ca index, X ray, and Mg ratio. (Annual tick marks correspond to January 1 of each year.)

with only minor enhancements found during sunspot maximum times, the other solar variables, especially Ca plage index and X ray intensity depict clear 13.5-day periodicity activations. Most of these activations occur around sunspot maxima, either in ascending phase (1979 and 1989) or early descending phase (1982 and 1991). The enhancement in 1979 was also among the strongest found by *Bobova and Stepanian* [1994], who studied spectral peaks of the background solar magnetic field and plage power. Mg ratio attains rather weak intensities, but the largest activation is seen in 1979 and coincides with the activation in Ca

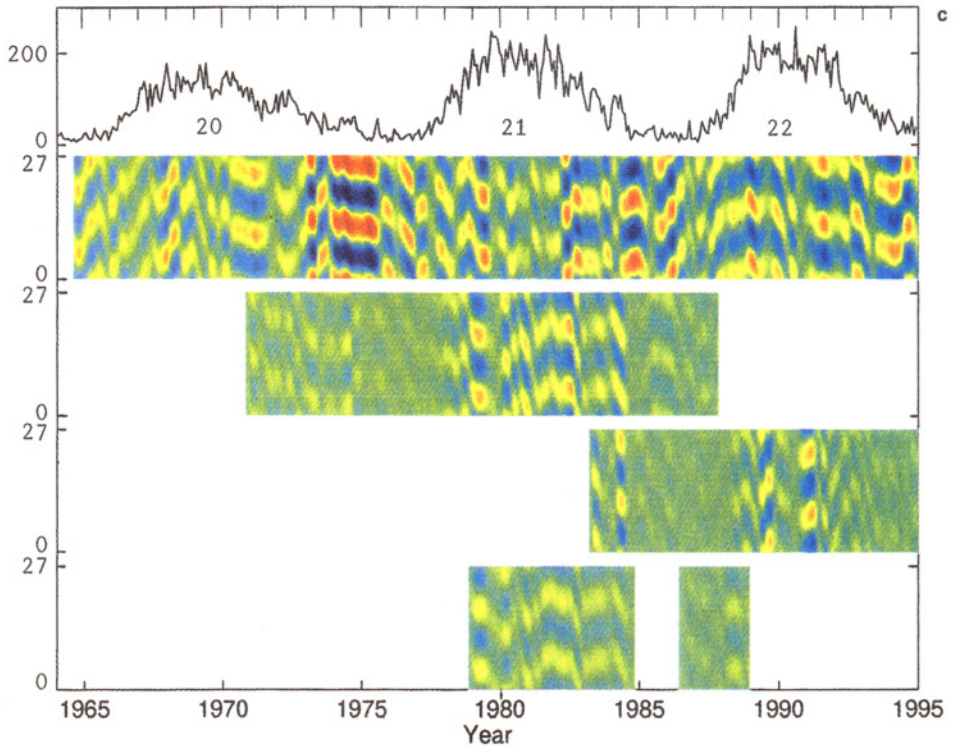

Plate 1. (continued)

index. One activation is found in the late declining phase in 1984. Note also that Ca index and X ray are then found to be in antiphase with each other. This is in accordance with the fact [*Donnelly and Puga*, 1990] that X ray maximum is obtained when the two sources are close to solar limbs rather than in the central meridian. Details like this give strong support for the method and results presented in Plates 1a-1c.

As seen in Plate 1c, there is hardly any 13.5-day periodicity observed in solar variables during the main 13.5-day enhancements of SW speed, demonstrating the difference between the chromospheric and heliospheric (or geomagnetic) 13.5-day periodicities, contrary to earlier claims [*Rangarajan*, 1991]. Rather, our results show that the two active solar longitudes do not generally coincide with and thus are not directly responsible for two-stream structures. Out of the five largest activations in any of the three solar variables, only the one in 1982 is seen as a subdominant activation in Plate 1a. (Furthermore, comparing with IMF sector component in Plate 1b, one can find that the solar 13.5-day enhancements do not seem to correspond to the main four sector structures either.)

5. Discussion

5.1. Method and Effect of Data Gaps

As mentioned above, SW and IMF variables suffer from serious data gaps. The overall coverage of SW and IMF was about 70-75%. However, there were a few long periods with 100% SW data coverage. One occurred during the most intense two-stream structure in 1974-1975. Figure 4 depicts SW speed in 1974. A dominant 13.5-day periodicity is clearly visible in the time series of daily averaged raw data, giving the magnitude of the largest 13.5-day enhancements and providing further evidence that results presented above are indeed real and not, for example, artefacts of the method.

Solar wind and IMF were often monitored by one satellite only, which imposes repetitive data gaps when the satellite stays within the Earth's magnetosphere, unable to measure direct SW. The orbital period (12.5 days) of IMP 8, responsible for SW and IMF observations as the only spacecraft for years, is quite close to the periodicity studied in this paper. Thus one might suspect that the power at about 13.5 days could rather be due to these repetitive data gaps (or sampling) on a signal which, instead, has

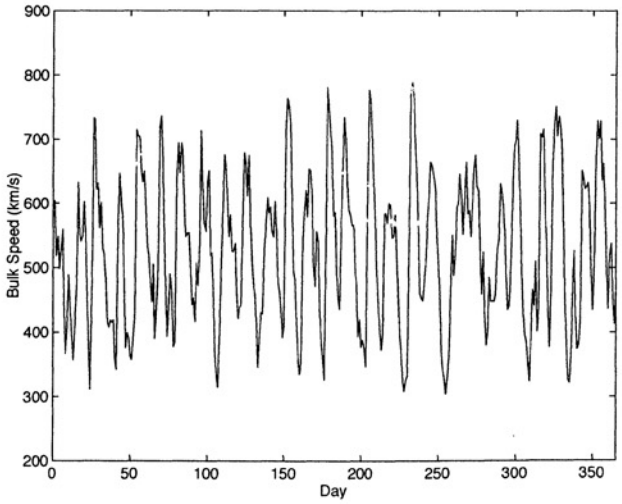

Figure 4. The daily averaged values of solar wind speed in 1974.

a periodicity of 27 days. Therefore we have simulated the effect of such repetitive data gaps on a 27-day signal. We launched a 27-day sine function with an amplitude of one unit and an average value of three units, and added a Gaussian noise with a unit standard deviation to it. (These numbers correspond roughly to noisy SW speed, typically a few standard deviations above zero.) Then we introduced the "IMP 8 window function" with 4-day (the average gap length) gaps repeating every 12.5 days, that is, imposed repetitive gaps in the "data." Figure 5a depicts the power spectrum of this windowed signal which has indeed a dominant peak at 12-13 days, even larger than the original 27-day signal.

However, this does not correspond to the way we treated the data. Instead, let us first subtract the average (or trend) from the data, and then impose the repetitive gaps in it. The corresponding power spectrum is given in Figure 5b, and shows a major peak at 27 days but no significant power at 12-13 days. Finally, Figure 5c depicts the power spectrum obtained after we first subtracted the average, then introduced the data gaps, and finally interpolated linearly over the data gaps (instead of setting them to zero). This procedure is exactly the method adopted in the paper. The power spectrum in Figure 5c is even more concentrated around 27 days than in Figure 5b (or Figure 5a), with very little power remaining at around 12-14 days (suppressed in both cases by at least 15 dB with respect to 27-day peak). Furthermore, spurious background peaks (due, for example, to finite length effects), like the one at about 8 days seen in Figure 5b, are also suppressed in Figure 5c.

The lesson from this simulation experiment is evident: filling all data gaps with a value (e.g., zero) which is far away from the average leads to a spurious peak (with harmonics) in the power spectrum at the gap repetion period. Filling the gaps with the average or, equivalently, removing the average (or trend) from the data and setting data gaps to zero will remove this peak and its harmonics. Even better, interpolating over the gaps will enhance the signal by reducing background power. Actually, the only effect of SW and IMF data gaps is to decrease (not increase) the overall 13.5-day power.

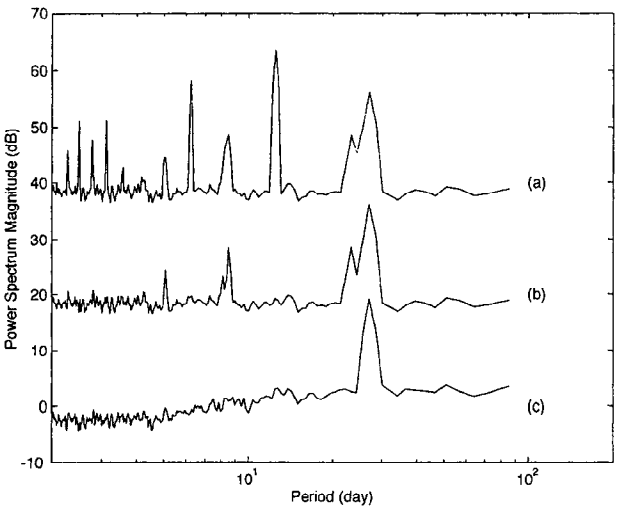

Figure 5. Power spectra of the simulated 27-day signal with 4-day gaps repeating every 12.5 days for (a) raw data with gaps; (b) data with gaps filled by average; (c) data with gaps filled by linear interpolation.

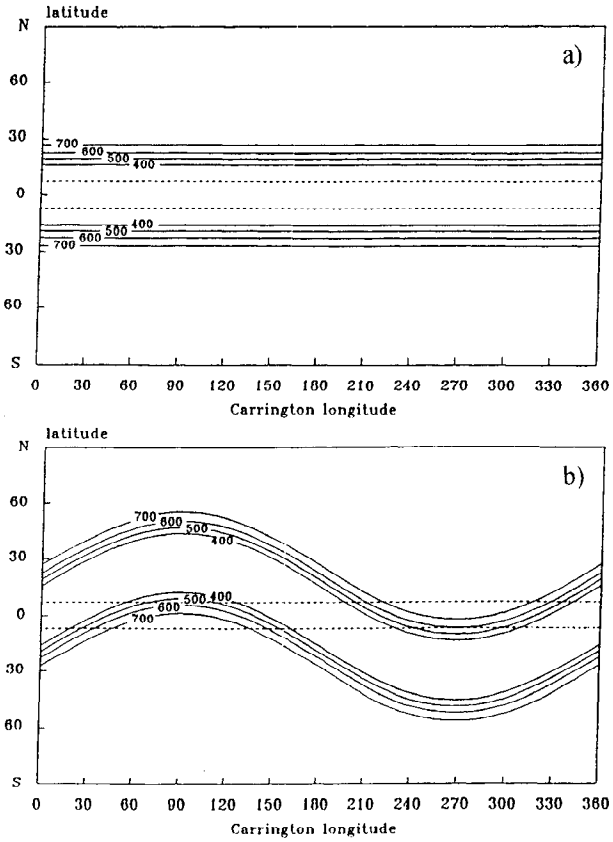

Figure 6. Model for SW speed distribution in case of a flat heliosheet when (a) the solar dipole axis is aligned with the solar rotation axis; (b) the dipole is tilted with respect to the rotation axis. The x axis gives the Carrington longitude, and y axis gives the heliographic latitude. The Earth's orbit close to autumn (spring) equinox is shown as the upper (lower) dashed line.

5.2. Tilted Dipole Model and Tilt Dynamics

Let us consider a situation [*Hakamada and Akasofu*, 1981; *Zhao and Hundhausen*, 1981] where the heliosheet is flat and perpendicular to the solar dipole axis, and where SW speed has its minimum (about 400 km/s) in the heliosheet, increases until about 30 deg of heliomagnetic latitude and attains a constant value (about 700 km/s) above it. The Carrington map representation of this model is shown in Figure 6a for the case when solar dipole axis is aligned with solar rotation axis. In Figure 6b the dipole is tilted with respect to rotation axis. The path of the Earth (traveling from right to left during one solar rotation) is represented by the upper (lower) dashed line close to autumn (spring) equinox when the Earth reaches the highest heliographic latitudes in the northern (southern) solar hemisphere. When the solar dipole is tilted enough, the Earth encounters two high-speed SW streams during one solar rotation. This model provides a simple and natural explanation for the 13.5-day periodicity of SW speed in near-Earth space. It is also valid for many other heliospheric variables, with proper modifications included; for example, the ion density has a maximum rather than a minimum at the heliosheet [see, e.g., *Mihalov et al.*, 1990; *Summanen et al.*, 1993], and thus it has a negative heliomagnetic latitudinal gradient, which gives a phase difference of about 180 deg with SW speed.

Accordingly, the occurrence of intervals of strong 13.5-day periodicity, that is, two-stream structures, requires that the heliosheet is sufficiently flat and tilted. Such a situation is called the excursion phase of solar cycle in the two hemisphere model [*Saito*, 1989]. The structure of the heliosheet and the properties of plasma around the ecliptic are closely connected with the development of polar coronal holes (for a review and references, see, for example, *Kojima and Kakinuma*, [1987, 1990]. Polar coronal holes and regions of high SW speed vary dramatically over the solar cycle, expanding toward the heliomagnetic equator in the declining phase and contracting in the ascending phase. Thus, in the declining phase, the width of the equatorial low-speed belt decreases and large heliomagnetic latitudinal gradients, gradients perpendicular to the heliosheet are formed at the boundary of the high-speed and low-speed regions (for a review of observations, see, for example, *Newkirk and Fisk* [1985] and *Rickett and Coles* [1991]). In maximum sunspot years the coronal holes have retreated back to the poles (or do not exist at all), and therefore no stable regions of high-speed SW exist at the ecliptic and speed gradients around the heliosheet are smaller than in late declining phase. Also, the solar magnetic field and the heliosheet are strongly perturbed (even multiple heliosheets may occur). Therefore no sizable 13.5-day periodicity appears in the heliospheric variables during solar maximum years.

For the three solar cycles studied, intervals of strongest 13.5-day periodicity in heliospheric and geomagnetic variables were found in the late declining phase of the solar cycle. This is in good agreement with the above model and the development of solar corona over the solar cycle. Furthermore, it is known that the heliosheet was flat [see, e.g., *Kojima and Kakinuma,* 1990] and sizably tilted [see, e.g., *Wang*, 1993] during the two largest two-stream structures in 1974-1975 (by about 40°) and 1984 (about 25°). Even the subdominant 13.5-day activations in the earlier descending phase, for example, in 1973 and 1982, occur during a large dipole tilt of about 45° [*Wang*, 1993]. Thus conditions required for the tilted dipole model to produce the 13.5-day periodicity are verified.

We also note that the Carrington longitude presentation of Plate 1a allows us to determine the longitude of the solar dipole tilt from the phase of the 13.5-day activations. (Of course, Plates 1a-1c cannot separate between the two opposite directions. Moreover, the delay of about 3-4 days due to finite SW speed has to be taken into account.) Note also that the dipole tilt direction can abruptly change even by 90 deg during two successive activations (e.g., in 1973 and 1994). This implies considerable variability in the dynamics of solar activity causing the dipole tilt. Amplitudes of the 13.5-day activations in Plate 1a are related to the size of the dipole tilt angle. However, they also depend on the heliomagnetic latitude gradients of the various SW variables. Therefore the relation between the tilt angle and the amplitude of activations separated by a long time interval, in particular those occurring in different phases of the solar cycle or in different solar cycles, is not straightforward.

5.3. IMF Sector Structure and Alternate Models

We will now study the occurrence of different types of IMF sector structures and their connection to two-stream structures. In Plate 2 we have plotted amplitudes of the 27-day periodicity and its harmonics (from second to sixth) for three variables: SW speed, Kp index, and IMF sector component. The harmonics

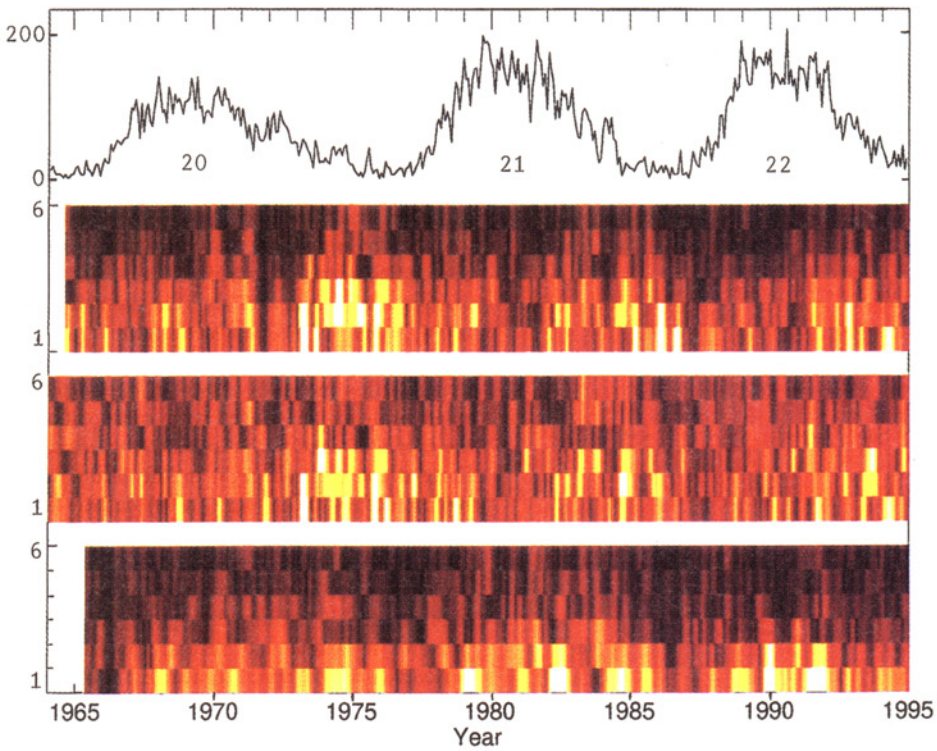

Plate 2. (top) Sunspot numbers averaged over one Carrington rotation, and the three colour plots depict amplitudes of the 27-day periodicity and its harmonics for three variables (from top to bottom): SW speed, Kp index, and IMF sector component. Amplitude of the 27-day periodicity (marked by 1) is given as the lowest row in each plot, the second and higher harmonics up to the sixth harmonic above it (marked by the respective number). Highest intensities are painted in light yellow and lowest in dark brown.

were computed for every 27-day interval by applying a multiband pass filter, each band passing only one of the harmonics of the 27-day variation. The 27-day periodicity amplitude is given as the lowest row in each panel, with the second harmonic (i.e., the 13.5-day periodicity) and higher harmonics above it successively. Amplitudes are given in color scale with highest intensities painted light yellow and lowest dark brown.

The two upper color panels in Plate 2 have a fairly similar overall structure, in agreement with the above discussed correlation between SW speed and Kp index. Their 13.5-day periodicity intensities (second row from below) reproduce the results of Plate 1a. Many of the structures in the fundamental and even in higher harmonics are similar for these two variables. Note also that the 13.5-day periodicity for SW speed and Kp index attains comparable overall intensities with the fundamental 27-day periodicity, in agreement with power spectrum results of section 3. Furthermore, during the largest two-stream structures seen in Plate 1a, the 13.5-day periodicity clearly surpasses the simultaneous intensity of the 27-day periodicity, verifying the fact that the 13.5-day periodicity is not just a numerical artefact of 27-day recurrency.

The IMF sector component (lowest panel in Plate 2) has most power in the fundamental, corresponding to the dominance of two sector IMF structures. In particular, a two sector structure was prevailing during the major two-stream structures (e.g., in 1974-1975 and 1984). However, the reverse is not true, that is, there are intervals of two-sector IMF structure with little or practically no 13.5-day activity observed in SW speed or Kp index. These intervals are found fairly close to sunspot maximum, either in the ascending (e.g., in 1979), early descending phase (1982) or at maximum (1990). It is known since long [*Davis*, 1965; *Davis et al.*, 1966] that high-speed streams have a preference for a definite IMF polarity, either toward or away from the Sun. Accordingly, our observations show that the two streams come from regions of opposite polarities and disagree with the view presented, for example, by *Gonzalez et al.* [1993] that the 13.5-day periodicity of geomagnetic activity is due to multiple sector IMF structure. Note also that while in SC 20 there was only one long period of two sector structure in the late declining phase, the other two cycles had two or three large two sector structures, some in the ascending, others in the descending phase. This shows that there are interesting differences in the evolution of IMF sector structure between the three cycles studied.

We also note of an alternate way to produce two-stream structures (13.5-day periodicity) whereby the solar coronal holes are asymmetric with two "tongues," about 180° apart in longitude, extending down to the ecliptic from the same pole. In such a case, however, the heliosheet would have a quadrupole, not dipolar, structure. Thus such an asymmetric corona is excluded as a significant contribution to 13.5-day periodicity. Furthermore, in such a model, it would be difficult to explain separate but closely following two-stream structures which are in antiphase with each other, as, for example, the two activations in 1973 or in 1994 (see Plate 1a). The development of coronal holes is clearly slower than required by this observation. On the other hand, the change of solar dipole tilt may well be fast enough to allow such a behavior.

5.4. IMF Radial Magnitude and Corotating Interaction Regions

It is well known that IMF intensity has a sharp maximum at a corotating interaction region (CIR) [*Burlaga and King*, 1979] (for a review, see, e.g., *Hakamada and Akasofu* [1982]) between a high speed and a low speed stream. The increase of IMF magnitude due to CIR is larger during the late declining phase of solar cycle than its increase with heliomagnetic latitude. In the tilted dipole model (see Figure 6b) this means that maximum IMF magnitudes are found in the region of large SW speed gradients, not at the highest heliomagnetic latitudes where highest SW speeds are found. Accordingly, the time of maximum IMF magnitude is shifted with respect to maximum SW speed. This is clearly seen in the filtered CCF between SW speed and IMF radial magnitude (Figure 3b). Maximum correlation was found 3 days before SW speed ACF maximum, in agreement with IMF maximum being at the leading edge (forward shock) of CIR. Moreover, the fact that geomagnetic activity leads SW speed but lags IMF magnitude supports the result [see, e.g., *Crooker and Cliver*, 1994] that peak geomagnetic activity is found in region of compressed IMF and increasing (but not peak) SW speed.

As already mentioned in section 4, the occurrence and relative power of the 13.5-day enhancements of radial IMF magnitude have a somewhat different distribution over the solar cycle than, for example, SW speed, attaining more power around sunspot maximum times (Plate 1b). It is interesting to note that the 13.5-day activations of radial IMF magnitude in 1970, 1979, and 1989 coincide exactly with the turn of the solar dipole whence increased values of horizontal magnetic field at solar surface are found [see, e.g., *Wang*, 1993]. At the time of dipole turn, the solar magnetic poles are close to the ecliptic, resulting in increased 13.5-day variation of solar radial magnetic field. Also, IMF had a two-sector structure during these and other main 13.5-day activations of radial IMF magnitude (compare lowest panel of Plate 1b and lowest row of Plate 2).

5.5. Length of 13.5-Day Activations

As discussed above, even the longest periods of two-stream structure (up to nearly 2 years) were found to consist of separate activations with a length of a few (about 4) solar rotations. Also, the other, separate activations of two-stream structure had approximately the same length. It is interesting to note that this length for two-stream structures coincides quite well with the observation made in Figure 2a that enhanced 27-day periodicity lasts for about 3-4 solar rotations. This equality can be understood in terms of the evolution of the solar dipole tilt which determines the occurrence of both periodicities.

Note also that the length of the (heliospheric) two-stream structures is approximately the same as that of the 13.5-day periodicity activations of solar variables. This indicates that the 13.5-day periodicity observed on solar surface and in the dipole tilt may still have a related dynamical origin. Recently, *Pap et al.* [1990] observed the 13.5-day periodicity, for example, in the projected areas of developing complex sunspot groups. However, no periodicity was found in the areas of old decaying sunspot groups. This shows that the 13.5-day periodicity observed on solar surface comes from two magnetically active solar regions (separated by about 180° in longitude). Thus the solar dynamics related to the development of large magnetically active regions is probably responsible for both solar 13.5-day periodicity and dipole tilt.

The IMF structures (see Plate 2), in particular the two sector structures, seem to be about twice longer than the SW two-stream structures. This is in accordance with the results based on the ACF of IMF sector component in section 3 (Figure 2b) and can easily be understood in terms of the tilted dipole model. Namely, during a small dipole tilt, the two-sector structure may

well prevail, but the two-stream structure may not be observed because of small gradients near the heliosheet. Note also that the longer duration of four-sector IMF structures was already seen in the fact that the 13.5-day activations of IMF sector component in Plate 1b were longer than those in Plate 1a.

5.6. Dst and Recurrent Storms

We have also studied the 13.5-day recurrency of the Dst parameter that reflects the Earth's ring current and the dynamics of magnetic storms. However, the 13.5-day periodicity of Dst index was much weaker than, for example, that of Kp index. Geomagnetic storms are, in simple terms, produced by the effect of two parameters with different periodicity properties: the negative IMF z component (no 13.5-day periodicity) and the large solar wind pressure (a clear 13.5-day periodicity). Their overall effect can explain the lack of significant 13.5-day periodicity for Dst.

This means that two-stream structures do not often include two large geomagnetic storms during one Carrington rotation, but only one (mostly from the hemisphere with favored IMF sector [*Russell and McPherron*, 1973]), the other hemisphere producing more restricted geomagnetic activity, that is, substorms. However, since all indices (Kp, aa, C9) of global geomagnetic activity demonstrate clear 13.5-day periodicity, the activity from the less favored hemisphere is fairly sizable as well. This is possible, for example, by the fact that sizable fluctuations due to interplanetary Alfvén waves [*Hakamada and Akasofu*, 1982] occur in IMF z component which balance the geoeffectivity differences between the two hemispheres. These fluctuations may also be partly responsible for the observed noisy structure of the IMF z component ACF (Figure 2b).

6. Conclusions

We have studied the occurrence of the 13.5-day quasi-periodicity over the last three solar cycles, including many solar wind, IMF, geomagnetic activity, and a number of solar chromospheric variables. Using a filtering technique, we were able to extract the detailed temporal structure of this periodicity. The largest enhancements of this periodicity are found in the late declining phase of solar cycle in case of heliospheric variables and around sunspot maxima in case of solar variables. Except for one, all the main 13.5-day activations occur at different times for these two groups of variables.

The main 13.5-day activations of heliospheric variables denote intervals of two high speed SW streams, and can be explained in terms of the tilted solar dipole model when the heliosheet is sufficiently flat and tilted. We noted that independent observations verify these conditions, that is, that the heliosheet was indeed flat and tilted during at least the largest two-stream structures. On the other hand, the occurrence of intervals of 13.5-day periodicity for solar variables verifies the previous observations of the existence of two active solar longitudes, now found to be active mainly around sunspot maximum times.

The Carrington longitude presentation used in Plate 1 allowed us to locate the longitude of solar dipole tilt from the phase of the 13.5-day periodicity. We noted that the longitudinal position of the solar tilt can change even by 90 deg during two successive activations, implying considerable variability in the dynamics of the solar activity causing the dipole tilt.

We find that, contrary to some recent suggestions [*Gonzalez et al.*, 1993], the 13.5-day periodicity of heliospheric and geomagnetic variables is not due to multiple IMF sector structure but occurs during two sector structure. Thus, for example, an asymmetric corona with two polar holes, originating from the same pole, separated by about 180° in longitude and leading to multiple IMF sector structure, is not the main cause for 13.5-day periodicity.

Even the longest two-stream structures, for example, the one lasting nearly 2 years in 1974-1975, are found to consist of separate activations. The activations have a typical length of a few (about 4) solar rotations only. Moreover, enhanced 27-day periodicity in heliospheric and geomagnetic variables lasts for roughly equally long. This can be understood by the development of the solar dipole tilt, affecting both of these periodicities. However, the IMF structures were found to be nearly twice as long, about 7-8 solar rotations. This is due to the fact that even quite small dipole tilt angles can sustain a two-sector pattern, although no two stream structure is observed because of small speed gradients near the heliosheet.

Despite the very different overall occurrence over the solar cycle, one interval of enhanced 13.5-day periodicity was found in the early declining phase in 1982, which was common to both solar, heliospheric and geomagnetic parameters. *Pap et al.* [1990] suggest that the solar 13.5-day periodicity comes from two new magnetically active solar regions, about 180° apart in longitude. Because the solar dipole tilt is also related to developing large-scale magnetic regions, the 13.5-day activation in 1982 may be due to magnetic regions which are responsible for both chromospheric activity and the dipole tilt. We also noted of the approximately similar length of the heliospheric (and geomagnetic) and solar 13.5-day activations which also supports the idea of a similar dynamical behavior between the two groups of 13.5-day periodicity.

The results on the recurrent properties presented in this paper can provide increased accuracy for predictions of space weather and geomagnetic activity level and could be useful in relevant computer programs and other methods. We would also like to note that the two-stream structures can be used as a more workable and reliable definition for the solar excursion phase than the 27-day periodicity, since they better correspond to the related requirements.

Acknowledgments. We thank K. Hakamada and T. Saito for useful discussions and T. Nygrén and I. Usoskin for comments. We are greatful to A. Lazarus, R. Lepping and J. King for providing the SW and IMF data available, to P. Cugnon for providing us with sunspot numbers and the referees for suggesting a number of useful additions which greatly increased the extent and quality of the paper. The solar data were kindly provided by the NOAA. Ms L. Kalliopuska is acknowledged for efficient help in proof correction and layout production, and Ms M. Kultima for librarial help. We gratefully acknowledge financial support by the Centre for International Mobility (CIMO), Finland, the Academy of Finland, the Hungarian Space Agency for the Hungarian Space Weather Project, and Hungarian National Science Foundation for the project 1171.

The editor thanks Aaron Barnes and another referee for their assistance in evaluating this paper.

References

Altschuler, M. D., D. E. Trotter, and F. Q. Orrall, Coronal holes, *Sol. Phys.*, *26*, 354-365, 1972.

Bai, T., Distribution of flares on the Sun: Superactive regions and active zone of 1980-1985, *Astrophys. J.*, *314*, 795-807, 1987.

Bame, S. J., J. R. Asbridge, W. C. Feldman, and J. T. Gosling, Solar cycle evolution of high-speed solar wind streams, *Astrophys. J.*, *207*, 977-980, 1976.

Bartels, J., Terrestrial magnetic activity and its relations to solar phenomena, *J. Geophys. Res.*, *37*, 1-52, 1932.

Bartels, J., Twenty-seven day recurrencies in terrestrial-magnetic and solar activity, 1923-1933, *J. Geophys. Res., 39*, 201-202, 1934.

Bartels, J., Solar radiation and geomagnetism, *J. Geophys. Res., 45*, 339-343, 1940.

Bobova, V. P., and N. N. Stepanian, Variations of the magnetic field of the Sun and the Earth in 7-50 day periods, *Sol. Phys., 152*, 291-296, 1994.

Broun, J. A., On the variations of the daily mean horizontal force of the Earth's magnetism produced by the sun's rotation and the moon's synodical and tropical revolutions, *Philos. Trans. R. Soc. London, 166*, 387-404, 1876.

Bruzek, A., The localization of Bartel's M-regions, *Z. Naturforsch. A, 7*, 708-711, 1952.

Burlaga, L. F., and J. King, Intense interplanetary magnetic fields observed by geocentric spacecraft during 1963-1975, *J. Geophys. Res., 84*, 6633-6640, 1979.

Burlaga, L. F., and R. P. Lepping, The causes of recurrent geomagnetic storms, *Planet. Space Sci., 25*, 1151-1160, 1977.

Chree, C., and J. M. Stagg, Recurrence phenomena in terrestrial magnetism, *Philos. Trans. R. Soc. London, Ser. A, 227*, 21-62, 1927.

Coles, W. A., Interplanetary scintillation, *Space Sci. Rev., 21*, 411-425, 1978.

Courtillot, V., and J. L. Le Mouel, Time variations of the Earth's magnetic field: From daily to secular, *Annu. Rev. Earth Planet. Sci., 16*, 389-476, 1988.

Crooker, N. U., and E. W. Cliver, Postmodern view of M-regions, *J. Geophys. Res., 99*, 23,383-23,390, 1994.

Davis, L., Jr., Mariner 2 observations relevant to solar fields, in *Stellar and Solar Magnetic Fields*, edited by R. Lüst, pp. 202-207, North-Holland, New York, 1965.

Davis, L., Jr., E. J. Smith, P. J. Coleman Jr., and C. P. Sonett, Interplanetary magnetic field measurements, in *The Solar Wind*, edited by R. W. Mackin and M. Neugebauer, pp. 35-52, Pergamon, Tarrytown, N. Y., 1966.

Delouis, H., and P. N. Mayaud, Spectral analysis of the geomagnetic activity index aa over a 103-year interval, *J. Geophys. Res., 80*, 4681-4688, 1975.

Dessler, A. J., and J. A. Fejer, Interpretation of Kp index and M-region geomagnetic storms, *Planet. Space Sci., 11*, 505-511, 1963.

Donnelly, R. F., Uniformity in solar UV flux variations important to the stratosphere, *Ann. Geophys., 6*, 417-424, 1988.

Donnelly, R. F., and L. C. Puga, Thirteen-day periodicity and the center-to-limb dependence of UV, EUV, and X-ray emission of solar activity, *Sol. Phys., 130*, 369-390, 1990.

Donnelly, R. F., D. F. Heath, J. L. Lean, and G. J. Rottman, Differences in the temporal variations of solar UV flux, 10.7-cm solar radio flux, sunspot number, and Ca-K plage data caused by solar rotation and active region evolution, *J. Geophys. Res., 88*, 9883-9888, 1983.

Donnelly, R. F., J. W. Harvey, D. F. Heath, and T. P. Repoff, Temporal characteristics of the solar UV flux and He I line at 1083 nm, *J. Geophys. Res., 90*, 6267-6273, 1985.

Donnelly, R. F., H. E. Hinteregger, and D. F. Heath, Temporal variations of solar EUV, UV, and 10830-Å radiations *J. Geophys. Res., 91*, 5567-5578, 1986.

Fenimore, E. E., J. R. Asbridge, S. J. Bame, W. C. Feldman, and J. T. Gosling, The power spectrum of the solar wind speed for periods greater than 10 days, *J. Geophys. Res., 83*, 4353-4357, 1978.

Fraser-Smith, A. C., Spectrum of the geomagnetic activity index Ap, *J. Geophys. Res., 77*, 4209, 1972.

Gonzalez, A. L. C., W. D. Gonzalez, S. L. G. Dutra, and B. T. Tsurutani, Periodic variation in the geomagnetic activity: A study based on the Ap index, *J. Geophys. Res., 98*, 9215-9231, 1993.

Gosling, J. T., and S. J. Bame, Solar wind variations 1964-1967: An autocorrelation analysis, *J. Geophys. Res., 77*, 12-26, 1972.

Gosling, J. T., J. R. Asbridge, S. J. Bame, and W. C. Feldman, Solar wind speed variations: 1962-1974, *J. Geophys. Res., 81*, 5061-5070, 1976.

Gosling, J. T., J. R. Asbridge, S. J. Bame, and W. C. Feldman, Preferred solar wind emitting longitudes on the Sun, *J. Geophys. Res., 82*, 2371-2376, 1977.

Greaves, W. M. H., and H. W. Newton, On the recurrence of magnetic storms, *Mon. Not. R. Astron. Soc., 89*, 641-646, 1929.

Hakamada, K., and S.-I. Akasofu, A cause of solar wind speed variations observed at 1 A.U., *J. Geophys. Res., 86*, 1290-1298, 1981.

Hakamada, K., and S.-I. Akasofu, Simulation of three-dimensional solar wind disturbances and resulting geomagnetic storms, *Space Sci. Rev., 31*, 3-70, 1982.

Hansen, R. T., S. F. Hansen, and C. Sawyer, Long-lived coronal structure and recurrent geomagnetic patterns in 1974, *Planet. Space Sci., 24*, 381-388, 1976.

Heath, D. F., Space observations of the variability of solar irradiance in the near and far ultraviolet, *J. Geophys. Res., 78*, 2779-2792, 1973.

Kiepenheuer, K. O., Solar activity, in *The Sun*, edited by G. P. Kuiper, Chap. 6, pp. 322-465, University Chicago Press, Chicago, Ill., 1953.

Kojima, M., and T. Kakinuma, Solar cycle evolution of solar wind speed structure between 1973 and 1985 observed with the interplanetary scintillation method, *J. Geophys. Res., 92*, 7269-7279, 1987.

Kojima, M., and T. Kakinuma, Solar cycle dependence of global distribution of solar wind speed, *Space Sci. Rev., 53*, 173-222, 1990.

Krieger, A. S., A. F. Timothy, and E. C. Roelof, A coronal hole and its identification as the source of a high velocity solar wind stream, *Sol. Phys., 29*, 505-525, 1973.

Lean, J. L., Estimating the variability of the solar flux between 200 and 300 nm, *J. Geophys. Res., 89*, 1-9, 1984.

MATLAB, *Signal Processing Toolbox for Use with MATLAB*, pp. 1(64)-2(175), MathWorks Inc., Natick, Mass., USA, 1994.

Maunder, E. W., Magnetic disturbances, 1882 to 1903 as recorded at the Royal Observatory Greenwich, and their associations with sunspots, *Mon. Not. R. Astron. Soc., 65*, 2-34, 1905.

Mihalov, J. D., A. Barnes, A. J. Hundhausen, E. J. Smith, Solar wind and coronal structure near sunspot minimum: Pioneer and SMM observations from 1985-1987, *J. Geophys. Res., 95*, 8231-8242, 1990.

Munro, R. H., and G. L. Withbroe, Properties of a coronal "hole" derived from extreme-ultraviolet observations, *Astrophys. J., 176*, 511-520, 1972.

Neupert, W. M., and V. Pizzo, Solar coronal holes as sources of recurrent geomagnetic disturbances, *J. Geophys. Res., 79*, 3701-3709, 1974.

Newkirk, G., Jr., and L. A. Fisk, Variation of cosmic rays and solar wind properties with respect to the heliospheric current sheet, 1, Five-GeV protons and solar wind speed, *J. Geophys. Res., 90*, 3391-3414, 1985.

Pap, J., W. K. Tobiska, and S. D. Bouwer, Periodicities of solar irradiance and solar activity indices, I, *Sol. Phys., 129*, 165-189, 1990.

Rangarajan, G. K., Variations in the strength of recurrent geomagnetic activity in solar cycles 11 to 21, *Earth Planet. Sci., 100*, 49-54, 1991.

Rickett, B. J., and W. A. Coles, Evolution of the solar wind structure over a solar cycle: Interplanetary scintillation velocity measurements compared with coronal observations, *J. Geophys. Res., 96*, 1717-1736, 1991.

Russell, C. T., and R. L. McPherron, Semi-annual variation of geomagnetic activity, *J. Geophys. Res., 78*, 92-108, 1973.

Saito, T., Solar cycle variation of solar, interplanetary and terrestrial phenomena, in *Laboratory and Space Plasmas*, Proceedings of the Second International Workshop on the Relation Between Laboratory and Space Plasmas, pp. 473-528, Springer-Verlag, New York, 1989.

Sargent, H. H., III, The 27-day recurrence index, in *Solar Wind-Magnetosphere Coupling*, edited by Y. Kamide and J. A. Slavin, pp. 143-148, Terra Sci., Tokyo, 1986.

Sawyer, C., High-speed streams and sector boundaries, *J. Geophys. Res., 81*, 2437-2441, 1976.

Shapiro, R., The inherent smoothing of whole-disk solar indices, *J. Geophys. Res., 70*, 245-246, 1965a.

Shapiro, R., Comparisons of power spectrums of artificial time series with spectrum of a solar plage index, *J. Geophys. Res., 70*, 3581-3586, 1965b.

Shapiro, R., and F. Ward, Three peaks near 27 days in a high-resolution spectrum of the international magnetic character figure Ci, *J. Geophys. Res., 71*, 2385-2388, 1966.

Sheeley, N. R., Jr., J. W. Harvey, and W. C. Feldman, Coronal holes, solar wind streams, and recurrent geomagnetic disturbances 1973-1976, *Sol. Phys., 49*, 271-278, 1976.

Singh, J., and T. P. Prabhu, Variations in the solar rotation rate derived from $Ca^{+}K$ plage areas, *Sol. Phys., 97*, 203-212, 1985.

Smyth, M. J., The corona and geomagnetism, *Observatory, 72*, 236-239, 1952.

Snyder, C. W., M. Neugebauer, and U. R. Rao, The solar wind velocity and its correlation with cosmic ray variations and with solar and geomagnetic activity, *J. Geophys. Res., 68*, 6361-6370, 1963.

Stimets, R. W., and C. Londono, Rotational modulation of Ca K flux ratio and sunspot number, *Sol. Phys., 76*, 167-180, 1982.

Summanen, T., R. Lallement, J. L. Bertaux, and E. Kyrölä, Latitudinal distribution of solar wind as deduced from Lyman alpha measurements: An improved method, *J. Geophys. Res., 98*, 13,215-13,224, 1993.

Veeder, M. A., Thunderstorms, auroras, and sunspots, *Am. Meteorol. J., 10*, 105-106, 1893.

Wang, Y.-M., On the latitude and solar cycle dependence of interplanetary magnetic field strength, *J. Geophys. Res., 98*, 3529-3537, 1993.

Ward, F. W., Jr., The variance (power) spectra of Ci, Kp, and Ap, *J. Geophys. Res., 65*, 2359-2375, 1960.

Ward, F., and R. Shapiro, Decomposition and comparison of time series of indices of solar activity, *J. Geophys. Res., 67*, 541-554, 1962.

Zhao, X.-P., and A. J. Hundhausen, Organization of solar wind plasma properties in a tilted, heliomagnetic coordinate system, *J. Geophys. Res., 86*, 5423-5430, 1981.

K. Mursula, Department of Physical Sciences, University of Oulu, FIN-90570 Oulu, Finland. (e-mail: Kalevi.Mursula@oulu.fi)

B. Zieger, Geodetic and Geophysical Research Institute, H-9401 Sopron, Hungary. (e-mail: zieger@ggki.hu)

(Received November 3, 1994; revised June 25, 1996;
accepted August 5, 1996.)